Investigating classifiers to decode execution and observation processes from intracranial signals

Kolly Florian, Mikami Sarah, Waridel Samuel

EPFL 2024 — CS433 ML4Science project — TNE Laboratory

Abstract—**Machine Learning (ML) techniques have become increasingly prominent in neuroscientific research. In particular, many studies investigated the use of ML tools on electroencephalography (EEG) recordings to classify or predict physical and mental states, often with great success. In this work, we apply ML models to different classification tasks: (i) Decoding execution from observation (ii) Decoding precision from power grasp in execution paradigm (iii) Decoding precision from power grasp in observation paradigm Our work is inspired by ongoing debate over the presence of an action-observation network in cortical signals. By characterizing these signals and applying classification models, we aim to uncover similarities and differences between execution and observation processes in upper limb movements, and to verify whether those characteristics are generalizable across different human subjects. Our findings demonstrate that ML models, including Deep Learning approaches, can effectively classify actions based on EEG features. However, we also observe that, for tasks where the subject is passively observing different movements, the models fail to capture the subtle differences in brain activity and therefore achieve low performances. These results highlight both the potential and challenges of using ML to decode neural activity using intracranial signals.**

I. INTRODUCTION

Machine Learning (ML) is has become a central tool in neuroscience, with applications in neural engineering (e.g. Brain-Computer Interfaces, BCIs [1]), diagnostics (see [2] for an overview) and fundamental research (such as the recent NeuroAI field). For instance, Jalilifard et al. [3] demonstrated the efficacy of Support Vector Machine classifiers in basic emotions recognition, while Bose et al. [4] used Random Forest classifiers to automate seizure detection in epileptic patients with high accuracy. Indeed, all major ML methods have been applied to neural signals classification [5].

In this work, we examine the applications of supervised ML models in three classification problems using stereo electroencephalography (sEEG) signals: i) distinguishing between the execution and observation of a movement; ii) differentiating between grasping a small object (precision grasp) versus a large object (power grasp); and iii) differentiating between observing the grasp of a small versus a large object. The sEEG data used here were collected from patients with electrodes in various brain regions. All patients were already implanted as partof their clinical treatment for a drug-resistant form of epilepsy.

Section II outlines the data acquisition process. In Section III, we describe the preprocessing of the sEEG signals and the extraction of relevant features. Section IV and Section V present the models applied to our classification problems and their performance. In Section VI, we explore the idea of using only Deep Learning (DL) methods to directly extract features from the EEG signal and train models. Finally, we discuss our results in Section VII and conclude in Section VIII.

II. DATA ACQUISITION

The dataset comprises signals recorded from four participants implanted with sEEG electrodes in distinct brain regions as part of their epilepsy treatment. During multiple experimental sessions, participants were instructed to either observe or execute specific motor tasks. These tasks involved two types of movements: a palmar grasp (power-based movement) and a pinch grasp (precision-based movement). Each session included multiple trials. Their structure is explained in Appendix X-B.

III. DATA ANALYSIS

In this section, we describe the preprocessing and analysis of the data. The dataset is a dictionary containing four subjects (named *s6*, *s7*, *s11* and *s12*). Each subject participated from one up to three sessions. During each session, the subjects completed 256 tasks, equally distributed as observation or execution tasks. The number and location of the channels are not identical across subjects, as they were implanted previous to the experiment.

A. Channel responsiveness

We first filtered the channels of interest: for a given channel and task, we define i) the *baseline signal* as the average signal across all task-specific trials in the one-second window between the start of the trial and the cue light turning on, and ii) the *effect signal* as the average signal across all task-specific trials in the one-second equally spaced window surrounding the moment the object is grasped, whether by the subject or the experimenter. Using Welch's method [6], we computed the power spectral density (PSD) for both the *baseline signal* and the *effect signal*. We then performed a t-test to compare the PSDs and define a *responsive channel* as a channel with a statistically

significative t-test ($\alpha < 0.05$, hyperparameter). This analysis was conducted separately for channels responsive during observation trials, execution trials, and responsive to both. As channels vary across subjects, the preprocessing was conducted individually for each subject.

B. Data preprocessing

The signals (one per channel) of each trial is preprocessed in three steps:

1) **Subsampling**: the signal is subsampled from 2048 Hz to 500 Hz to reduce the computational needs. Since the EEG data contains information up to approximatively 150 Hz, this subsampling respects the Nyquist criterion.
2) **Z-score correction**: Each EEG signal is normalized with Z-score normalization, calculated using the mean and standard deviation of the *baseline signal*.
3) **Resampling**: all trials are resampled to ensure they contain the same number of timepoints. The final number of sample was set to 1500.

C. Feature extraction

Participant with multiple sessions were handled as if they had a larger number of trials. Each task have it's own dataset based on the classification task to perform. For action recognition, all trials were taken and labeled as execution and observation trial. For movement recognition, trials were taken accordingly to the action type studied and labeled based on the movement type. For all dataset, the features were extracted in a similar way. For each responsive channels of a given task (see III-A), the trial signal was bandpass-filtered filter between the following frequency bands; alpha (8-12 Hz), beta (12-30 Hz), gamma (30-100 Hz) and theta (4-8 Hz). For each frequency band, the rectified envelope of the singal was calculated using the Hilbert transform. The trial was separated in windows of 1000 time point, separated by a step of 100 time point. The values of one window were summarized using the mean and the standard deviation. Finally, features from each responsive channels, each frequency bands and each time window were concatenated in a final dataframe.

IV. ACTION RECOGNITION

In this first classification task, we train and optimize different ML models to predict whether the participant was executing the movement or observing it. The analysis is restricted to channels responsive to both movements. Given the distinct nature of the tasks being compared, we anticipate strong performance across all models.

A. Responsivity of channels

The locations of the responsive channels is critical in understanding a potential action-observation network. To this end, we sorted the responsive channels in ascending order of the t-tests' p-value. For participant *s6*, Figure 1

shows the locations of the ten first responsive channels, respectively in the precentral gyrus (5), and the postcentral gyrus (5) over a total of 40 responsive channels. Table I shows the locations of the most responsive channels for all participants.
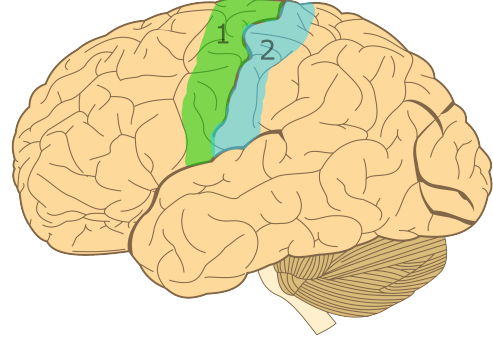

Figure 1. Locations of the ten most responsive channels in participant *s6*: The green area (1) represents the precentral gyrus, and the blue area (2) corresponds to the postcentral gyrus. Edited from Hugh Guiney, CC BY-SA 3.0 https://creativecommons.org/licenses/by-sa/3.0, via Wikimedia Commons

Part.	# channels	Main locations (# channels)
s6	40	prec. (5), postc. (5)
s7	26	prec. (7), postc. (1), cmf. (1), parso. (1)
s11	27	prec. (1), rmf. (1), sf. (5), WMpara. (2), para. (1)
s12	29	ins. (4), sp. (1), pc. (2), para. (1), postc. (2)

Table I
Number of responsive channels in total and location of the ten most responsive per participant. Appendix IV contains the list of acronyms

For this task we see that the regions vary quite a bit between participants. Participant *s6* has only two regions with responsive channels, while *s12* has five. But on the contrary, the number of responsive channels is quite similar for most participants, sitting around 30, with the exception of participant *s6* with 40 channels.

The regions with the most importance are similar across participants and are directly linked to movement (ex : prec.) or somatosensory information (ex : postc.). This makes sense as the task is linked with active hand movement and requires sensory feedback. It is interesting to note that some of the participants (*s11* and *s12*) have activity in areas that are more related to self-awareness and self-perception (ex: sf. and ins.), which could be much more linked to the observation trials.

TODO?

For channels where we have response for both ex & obs, are the responses congruent (similar pattern) or incongruent (different)?

B. Analysis of frequency bands

We investigate if specific frequency bands could gives more information than other and if there are differences across the action type. We trained the model with a dataset containing only features from a specific frequency band. We then compared the performance of the models across the different frequency bands (see Appendix 7). For action recognition, all models can detect the action type with high accuracy, regardless of the frequency band (above 75%). The best performance was obtained with delta and gamma frequency bands, with accuracies around 95%, which suggest that these bands are the most informative for differentiating observation from execution.

C. Baseline data

In order to verify the claim that channel responsiveness is a critical measure for selecting channels on which to compute the features, we also generated a list of channels that are not responsive, and computed features from them. We run each model on both sets of data, and a comparison is done in the results.

D. Models

To create and train the classical ML models, we adopted the well-known and performant Scikit-Learn library [7]. The Deep Learning models are developed using the PyTorch library [8]. We selected models based on the literature available on EEG analysis.

Logistic regression: Logistic regression (LR) is a computationally simple ML technique, and has previously used in EEG classification [9], [10].

SVM: We train two Singular Vector Machines (SVM) models, with and without PCA. SVM can handle high dimensional data, even for small datasets. Although more computationally than other methods, it is widely used in EEG classification with good results [11].

Random forest: Random Forest (RF) classifiers combine the output of multiple decision trees to reach a single result. Frequently used with a lower set of carefully crafted features (e.g. in [12] with 11 features), we hypothesize that we can also have interesting results using RF here.

MLP: In addition to traditional ML models, we also train Multilayer Perceptron (MLP) models. We chose to include MLP as it is widely used in EEG classification[1]. The main issue with MLP is that they are universal approximators and are thus prone to overfitting, especially for datasets as small as ours.

We try different MLP and select the best by using a validation subset. MLP models are trained for 10 epochs with batches of 4 datapoints. We use the AdamW optimizer, which directly applies weight decay (10^{-2}, hyperparameter)

---

[1]3'610 results for 'EEG MLP classification' on Google Scholar in 2024 at the time of writing

---

directly during the parameter update, leading to more consistent regularization and better generalization. The MLP is optimized and discussed only for participant *s6*.

E. Results

We tested the models on the same test set. As expected, all models obtained very high accuracies. When using non-responsive channels, we see a large drop in performance (although it is higher than chance). This confirmed our hypothesis that we can reduce significantly the number of features by first selecting responsive channels.

The MLP is also performing very well for participant *s6*: on the test set, we obtain an accuracy of 95% while the baseline is at 49%. The best model is also the simplest: two layers of 8 neurons each, with a learning rate of 10^{-1}.
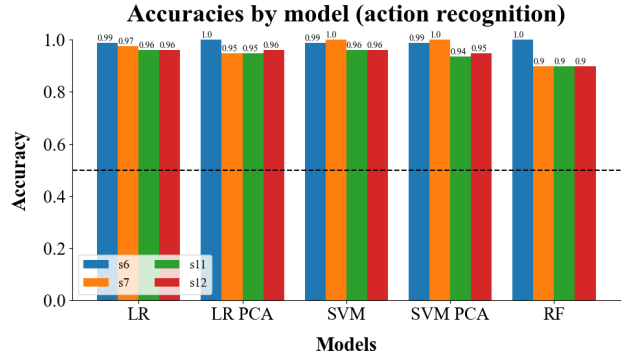

Figure 2. Accuracies by model and participant for the action recognition task: all models perform very well when trained on features extracted from responsive channels

F. Discussion

As expected, we obtain very good accuracies over all models and participants. Random forests see a small drop in performance: as explained above, this type of model could attain better accuracies when given carefully crafted features.

V. MOVEMENT RECOGNITION

For the second and third type of classification tasks, we analyze whether ML models are able to classify the type of movement done (precision grasp or power grasp) during execution and observation. We expect both tasks to be hard to learn. Observation, in particular, is a complex task, as the participant is simply seeing two different movements that have the same goal of lifting an object. In this part, we lessen the restrictions to select the *responsive channels*: it suffices for a channel to be responsive in execution or in observation respectfully to be included.

A. Responsive channels

The number of responsive channels and the locations of the ten most responsive channels for each participant are shown in Appendix II for execution and Appendix III for observation.

In both of these tasts, we see similar overall trends between all of the participants. Most channels are located in regions related to movement and somatosensory information such as the precentral gyrus (prec.) and the postcentral gyrus (postc.). Similarly to the first task, participant *s6* has areas linked very directly to hand movement, while participants *s11* and *s12* have activity in areas that are more related to self-awareness and self-perception (ex: sf. and ins.). This could explain a potential difference in interpretability of their data since they are much less directly linked to hand movement.

The number of responsive channels is quite different between participants and between the two tasks. The responsive channels are different in terms of location. We find some similarities but no clear pattern.

TODO?

For channels where we have response for both ex & obs, are the responses congruent (similar pattern) or incongruent (different)?

B. Analysis of frequency bands

As previoulsy with the action recognition task, the models was trained with features extracted from each frequency bands for both execution (see Appendix 8) and observation (see Appendix 9). The results are quite different from the action recognition task. The models are not able to capture the differences between the two types of movements, with accuracies barely above chance level. This suggests that the features extracted from the EEG signals are not able to capture the differences between the two types of movements.

C. Models

We use the same families of model as in the previous part for both classification in execution tasks and in observation tasks. We test the same hyperparameters sets for MLP, although these tasks might be significantly harder.

D. Results

As expected, our results are significantly lower in those tasks than in the first part. We also observe a drop in performance between execution and observation.

Execution trials: LR with and without PCA tends to perform better than the other models, and with more consistency across participants. SVM performs higher than average only for participant *s11*. RF was not able to capture the subtle differences in the features. Similarly, MLP on participant *s6* does not perform above chance.

Observation trials: Similarly as for the execution distinction, all models have low accuracy, barely performing better than chance. Except for participant *s11*, SVM is at chance level. LR performs slightly better than the other models. Again, all MLP models fail to capture meaningful information from our features.

E. Discussion

TODO SARAH Which freq. bands are important? Is it the same across subjects?

VI. PURE DEEP LEARNING APPROACH

Instead of extracting features on the responsive channels before training deep networks, one can ask whether the networks should learn to do that themselves. We explore this question in this section. We train two types of Convolution Neural Networks (CNN) directly on the trial signals. The hope is that the convolutional layers manage to extract important features from the signal, giving it as input to the subsequent MLP. In this section, we are not focusing on performance and thus wont optimize models. Instead, we are attempting new techniques as proof of concept.

A. 1D CNN

One-dimensional CNNs are composed of kernels that are convolved with a channel's signal directly. As they operate on data in one dimension, the input will be a tensor of size (N, C, L), where N is the batch size, C the number of (responsive) channels and L the fixed length of each trial. This is close to how we computed our features: supposing the same kernel size as the length of our moving averages, we would get the same features if the network learned moving averages too. Given this and the known power of CNNs, we expect this model to have the best performance. The caveat is overfitting, as we have small datasets.

B. 2D CNN

Two-dimensional CNNs are composed of 2D kernels that will operate on multiple channels at the same time. This means that we give as input a tensor of dimensions (N, C, H, W), with H the number of (responsive) channels and W the length of each signal. The use of naming dimensions H and W not arbitrary. Indeed, we can think of this superposition of channels as a picture, where each signal is a position on the y-axis and every timepoint a position on the x-axis.

C. Results

TODO FLORIAN The architectures of the CNNs used are detailed in Appendix X-G.

VII. DISCUSSION

TODO ALL

VIII. Conclusion

In this project, we used various ML models to analyze the classification accuracies of three distinct tasks. While every model was capable of classifying well the first task, the performance dropped when the differences in brain signals were more subtle. Our work therefore shows that ML models can already successfully be applied to (s)EEG signals without the need for handcrafted features, but they need clear differences in signal. Further experiments can be done on the models developed here to finetune them and verify whether they are able to achieve similar accuracy as in more distinct tasks or not. Additionally, more research is necessary on the preprocessing pipeline and feature extraction as to find optimal data to feed the models.

IX. Ethical risks

It is clear that the analysis of EEG and other brain signals present a unique set of ethical challenges. Given that we are not sharing the dataset for privacy concern, we will focus on this ethical risk in this brief analysis. EEG signals reveal information not only about the physical health of a subject, but also mental states, emotions and cognitive functions. With the popularization of such tools, we risk losing a fundamental right to mental privacy. This is not only true for emotions, but also religious and political opinions. For instance, neuropolitics[13] is a whole field of research that wishes to find the neural roots of our political beliefs. Prediction is just a step further, step that already stated with work such as [14] and [15].

As current methods require possible invasive electrodes, or to use expensive and complicated machines such as fMRI scanners, primarily patients ongoing clinical treatment and study subjects are affected by those risks at the moment. However, the potential violation of cognitive privacy underscores the need for robust privacy and anonymization measures when using EEG datasets. If not correctly established, third parties could gain valuable data on the private mental processes of a user and use it to their advantages. Companies such as Tesla or Meta already invested in such technologies, and not renowned for their privacy-oriented policies. The severity and ramifications of cognitive privacy violating in a large pool of user is hard to quantify, but without strict policies, the possibility of a future without private thought becomes alarmingly plausible.

Even without speculating about future developments in brain signal analysis, EEG signals are already used in identifying individuals. For example, tools for User Authentication via EEG signals already exists[16]. It is then clear that, when in possession of private EEG data, precautions must be taken to ensure that this data remains within the restricted pool of authorized researchers who have been granted access. In this project, we were careful not to upload this data on any online repository (e.g. GitHub), and we will not give the dataset to correctors outside the TNE laboratory. Moreover, we did not access any personal information from the participants involved.

Advanced methods exist to encrypt data while allowing computations on it[17]. Unfortunately, the time and scope of this project did not permit the implementation of such technologies.

X. Appendix

A. Experimental setup

The participants were asked to keep their hands on the resting positions. The led lights are used both to indicate who will realise the action and to specify which objects has to be grasped. A.) execution trial: the participant must pick the small green ball using a precise pinch grasp. B.) observation trial: the experimenter must pick the large red ball using a power grasp. C.) control action, not used in this project.
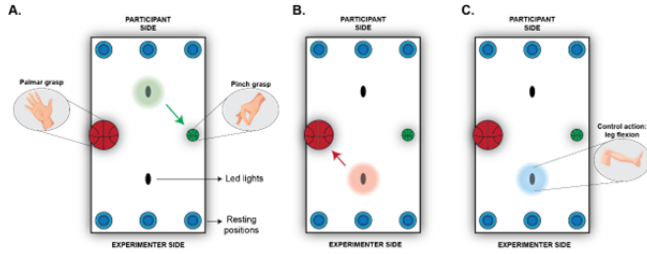

Figure 3. Experimental setup; courtesy of L. Pollina

B. Timeline

Each trial is structured as follows (see Appendix 4): execution trial begins with a start cue. One second later, a light cue signals the type of object (small or large) to be targeted. This light remains illuminated for 0.5 seconds before turning off. After an additional 1.5 seconds, a "go" signal prompts the participant to lift their hand from the resting position, grasp the indicated object, return it to its original location, and place their hand back in the resting position. Observation trials followed an identical structure, except that participants passively observed the experimenter performing the actions. A light cue indicated the participant's role (execution or observation) in each trial.

Figure 4. Timing of the trials: the areas shaded in grey indicates fixed timing, and the areas shaded in blue indicates timing that depends on the speed of execution of either the participant (execution) or the experimenter (observation); courtesy of L. Pollina

C. Responsive channels for movement recognition

Here, we show the locations of the ten responsive channels in the two movement recognition tasks. Appendix II is for the execution tasks, and Appendix III is for the observation tasks.

Part.	# channels	locations for execution (# channels)
s6	68	spm. (2), postc. (1), prec. (6), cmf. (1)
s7	48	postc. (1), th. (1), prec. (8)
s11	52	prec. (4), sf. (5), WMpara. (1)
s12	76	para. (1), pc. (3), postc. (2), sp. (1), ins. (3)

Table II
Number of responsive channels for execution trials and location of the ten most responsive per participant. Appendix IV contains the list of acronyms

Part.	# channels	locations for observation (# channels)
s6	51	postc. (6), prec. (4)
s7	33	cmf. (1), postc. (2), prec. (7)
s11	43	pren. (1), cmf. (1), para. (1), sf. (6), rmf. (1)
s12	48	para. (2), pc. (3), postc. (1), sf. (1), prec. (1), ins. (2)

Table III
Number of responsive channels for observation trials and location of the ten most responsive per participant. Appendix IV contains the list of acronyms

D. Acronyms

Appendix IV contains the list of brain regions' acronyms used in the report. It does not contain all the regions the participants had electrodes in, but only those relevant in our analyses.

Acronym	Corresponding region
cmf.	caudal middle frontal gyrus
ins.	Insula
para.	paracentral
parso.	parsopercularis
pc.	posterior cingulate
postc.	postcentral gyrus
prec.	precentral gyrus
pren.	precuneus
rmf.	rostral middle frontal
sf.	superior frontal gyrus
sp.	superior parietal gyrus
spm.	supramarginal
th.	thalamus
WMpara.	White Matter paracentral

Table IV
List of acronyms for the brain regions

E. Accuracies in movement recognition

The following graphs represent the accuracies obtained by model and by participant for the two movement recognition classification tasks. As mentioned in the main report, these accuracies are all low, due to the difficulty of finding neural differences between the compared tasks.
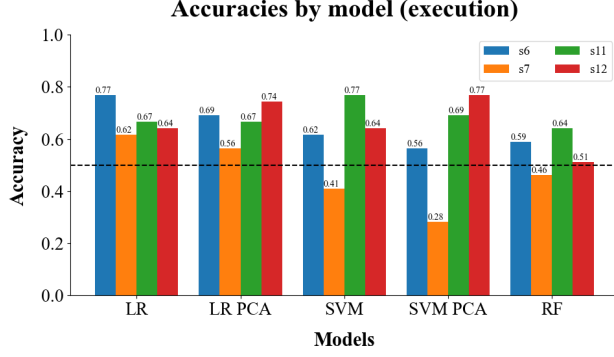
Figure 5. Accuracies by model and participant for the movement recognition task, executed by the subjects (execution)
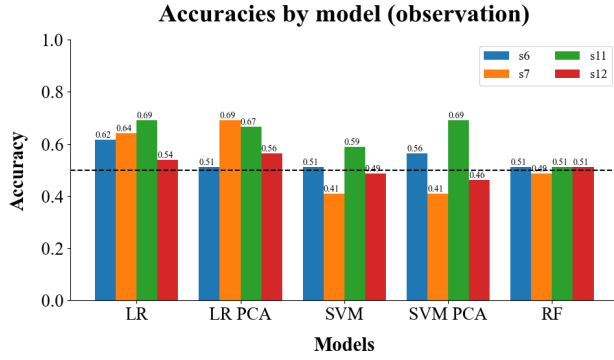

Figure 6. Accuracies by model and participant for the movement recognition task, executed by the experimenter (observation)

F. Analysis of accuracy by frequency bands

Here, we provide an analysis of the accuracies of our model based on which frequency band we give to compute the features.
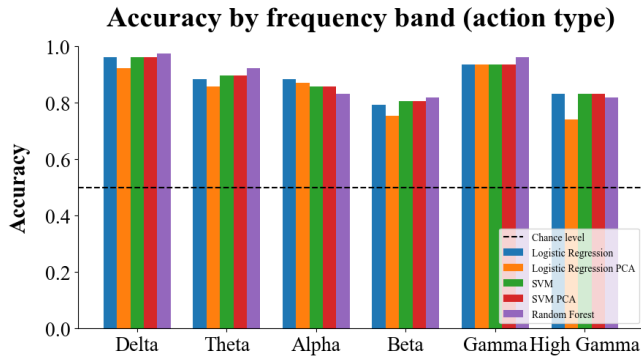

Figure 7. Accuracies by model and frequency band used for feature extraction, action recognition task on participant *s6*
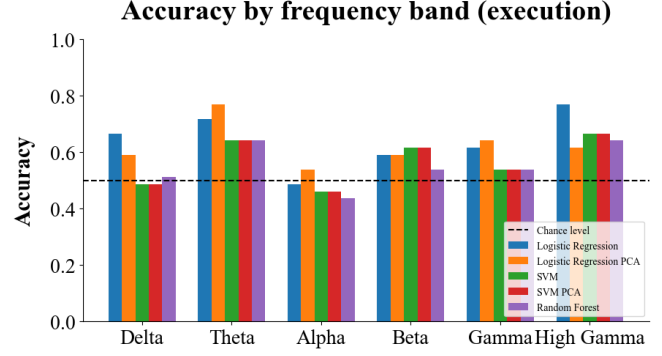

Figure 8. Accuracies by model and frequency band used for feature extraction, movement recognition task on participant *s6* (execution)
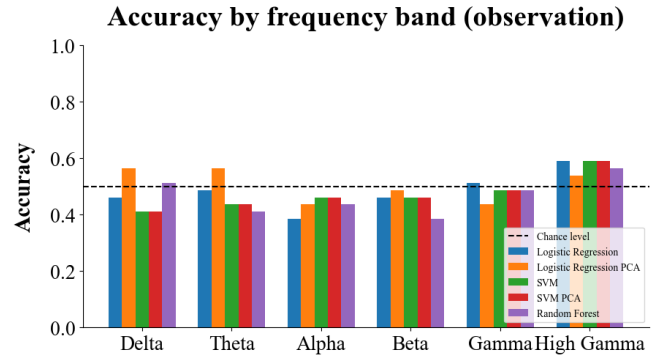

Figure 9. Accuracies by model and frequency band used for feature extraction, movement recognition task on participant *s6* (observation)

G. CNN architectures

2D CNNs: The 2D CNN architecture is as follows:

- Convolution layer: 2 channels, kernels of size 5×5, padding of 1, stride of size 3×3, ReLU
- Max-pooling layer: kernel of size 2×2
- Batch normalization
- Convolution layer: 4 channels, kernels of size 3×3, padding of 1, stride of size 3×3, ReLU
- Max-pooling layer: kernel of size 2×2
- Batch normalization
- Flattening
- Linear layer of 32 neurons, ReLU, dropout of 0.1
- Linear layer of 16 neurons, ReLU, dropout of 0.1
- Linear layer of 2 neurons, outputs the logits

We train all 2D CNNs with a learning rate of 0.001 over 10 epochs with a weight decay of 10 to avoid fast overfitting.

1D CNNs: The 1D CNN architecture is as follows:

- Convolution layer: 8 channels, kernel of size 10, padding of 1, stride of size 5, ReLU
- Max-pooling layer: kernel of size 2
- Batch normalization
- Convolution layer: 16 channels, kernel of size 50, padding of 1, stride of size 5, ReLU

- Max-pooling layer: kernel of size 2
- Batch normalization
- Flattening
- Linear layer of 64 neurons, ReLU, dropout of 0.1
- Linear layer of 32 neurons, ReLU, dropout of 0.1
- Linear layer of 2 neurons, outputs the logits

We train all 1D CNNs with a learning rate of 0.001 over 10 epochs with weight decay of 10 to avoid fast overfitting.

REFERENCES

[1] S. Vaid, P. Singh, and C. Kaur, "Eeg signal analysis for bci interface: A review," in *2015 Fifth International Conference on Advanced Computing & Communication Technologies*, 2015, pp. 143–147.

[2] S. Vieira, W. H. Pinaya, and A. Mechelli, "Using deep learning to investigate the neuroimaging correlates of psychiatric and neurological disorders: Methods and applications," *Neuroscience & Biobehavioral Reviews*, vol. 74, pp. 58–75, 2017. [Online]. Available: https://www.sciencedirect.com/science/article/pii/S0149763416305176

[3] A. Jalilifard, E. B. Pizzolato, and M. K. Islam, "Emotion classification using single-channel scalp-eeg recording," in *2016 38th Annual International Conference of the IEEE Engineering in Medicine and Biology Society (EMBC)*, 2016, pp. 845–849.

[4] S. Bose, V. Rama, N. Warangal, and C. Rama Rao, "Eeg signal analysis for seizure detection using discrete wavelet transform and random forest," in *2017 International Conference on Computer and Applications (ICCA)*, 2017, pp. 369–378.

[5] M.-P. Hosseini, A. Hosseini, and K. Ahi, "A review on machine learning for eeg signal processing in bioengineering," *IEEE Reviews in Biomedical Engineering*, vol. 14, pp. 204–218, 2021.

[6] O. M. Solomon, Jr, "Psd computations using welch's method. [power spectral density (psd)]," 12 1991. [Online]. Available: https://www.osti.gov/biblio/5688766

[7] F. Pedregosa, G. Varoquaux, A. Gramfort, V. Michel, B. Thirion, O. Grisel, M. Blondel, P. Prettenhofer, R. Weiss, V. Dubourg, J. Vanderplas, A. Passos, D. Cournapeau, M. Brucher, M. Perrot, and E. Duchesnay, "Scikit-learn: Machine learning in Python," *Journal of Machine Learning Research*, vol. 12, pp. 2825–2830, 2011.

[8] A. Paszke, S. Gross, S. Chintala, G. Chanan, E. Yang, Z. DeVito, Z. Lin, A. Desmaison, L. Antiga, and A. Lerer, "Automatic differentiation in pytorch," 2017.

[9] A. Subasi and E. Erçelebi, "Classification of eeg signals using neural network and logistic regression," *Computer Methods and Programs in Biomedicine*, vol. 78, no. 2, pp. 87–99, 2005. [Online]. Available: https://www.sciencedirect.com/science/article/pii/S0169260705000246

[10] R. Tomioka, K. Aihara, and K.-R. Müller, "Logistic regression for single trial eeg classification," in *Advances in Neural Information Processing Systems*, B. Schölkopf, J. Platt, and T. Hoffman, Eds., vol. 19.   MIT Press, 2006. [Online]. Available: https://proceedings.neurips.cc/paper_files/paper/2006/file/35937e34256cf4e5b2f7da08871d2a0b-Paper.pdf

[11] M. N. A. H. Sha'abani, N. Fuad, N. Jamal, and M. F. Ismail, "knn and svm classification for eeg: A review," in *InECCE2019*, A. N. Kasruddin Nasir, M. A. Ahmad, M. S. Najib, Y. Abdul Wahab, N. A. Othman, N. M. Abd Ghani, A. Irawan, S. Khatun, R. M. T. Raja Ismail, M. M. Saari, M. R. Daud, and A. A. Mohd Faudzi, Eds.   Singapore: Springer Singapore, 2020, pp. 555–565.

[12] C. Donos, M. Dümpelmann, and A. Schulze-Bonhage, "Early seizure detection algorithm based on intracranial eeg and random forest classification," *International Journal of Neural Systems*, vol. 25, no. 05, p. 1550023, 2015, pMID: 26022388. [Online]. Available: https://doi.org/10.1142/S0129065715500239

[13] D. Schreiber, "Neuropolitics: Twenty years later," *Politics and the Life Sciences*, vol. 36, no. 2, p. 114–131, 2017.

[14] G. Galli, D. Angelucci, S. Bode, C. De Giorgi, L. De Sio, A. Paparo, G. Di Lorenzo, and V. Betti, "Early EEG responses to pre-electoral survey items reflect political attitudes and predict voting behavior," *Scientific Reports*, vol. 11, no. 1, p. 18692, Sep. 2021. [Online]. Available: https://doi.org/10.1038/s41598-021-96193-y

[15] J. H. Yun, Y. Kim, and E.-J. Lee, "ERP Study of Liberals' and Conservatives' Moral Reasoning Processes: Evidence from South Korea," *Journal of Business Ethics*, vol. 176, no. 4, pp. 723–739, Apr. 2022. [Online]. Available: https://doi.org/10.1007/s10551-021-04734-2

[16] C. A. Fidas and D. Lyras, "A review of eeg-based user authentication: Trends and future research directions," *IEEE Access*, vol. 11, pp. 22 917–22 934, 2023.

[17] A. B. Popescu, I. A. Taca, C. I. Nita, A. Vizitiu, R. Demeter, C. Suciu, and L. M. Itu, "Privacy preserving classification of eeg data using machine learning and homomorphic encryption," *Applied Sciences*, vol. 11, no. 16, 2021. [Online]. Available: https://www.mdpi.com/2076-3417/11/16/7360